Impact of left bundle branch block on myocardial perfusion and metabolism: A positron emission tomography study

Ganna Degtiarova, MD,[a,b] Piet Claus, PhD,[c] Jürgen Duchenne, PhD,[c,d] Georg Schramm, PhD,[a] Johan Nuyts, PhD,[a] Hein J. Verberne, MD, PhD,[e] Jens-Uwe Voigt, MD, PhD,[c,d] and Olivier Gheysens, MD, PhD[a,b]

[a] Department of Imaging and Pathology, KU Leuven, Leuven, Belgium
[b] Nuclear Medicine and Molecular Imaging, University Hospitals Leuven, Leuven, Belgium
[c] Department of Cardiovascular Sciences, KU Leuven, Leuven, Belgium
[d] Department of Cardiovascular Diseases, University Hospitals Leuven, Leuven, Belgium
[e] Department of Radiology and Nuclear Medicine, Amsterdam UMC, location AMC, University of Amsterdam, Amsterdam, The Netherlands

Received May 30, 2019; Revised Aug 26, 2019; accepted Sep 10, 2019
doi:10.1007/s12350-019-01900-y

Background. **Better understanding of pathophysiological changes, induced by left bundle branch block (LBBB), may improve patient selection for cardiac resynchronization therapy (CRT). Therefore, we assessed the effect of LBBB on regional glucose metabolism, ^{13}N-NH$_3$-derived absolute and semiquantitative myocardial blood flow (MBF), and their relation in non-ischemic CRT candidates.**

Methods. **Twenty-five consecutive non-ischemic patients with LBBB underwent ^{18}F-FDG and resting dynamic ^{13}N-NH$_3$ PET/CT prior to CRT implantation. Regional ^{18}F-FDG uptake, absolute MBF, and late ^{13}N-NH$_3$ uptake were analyzed and corresponding septal-to-lateral wall ratios (SLR) were calculated. Segmental analysis was performed to evaluate ''reverse mismatch,'' ''mismatch,'' and ''match'' patterns, based on late ^{13}N-NH$_3$/^{18}F-FDG uptake ratios.**

Results. **A significantly lower ^{18}F-FDG uptake was observed in the septum compared to the lateral wall (SLR 0.53 ± 0.17). A similar pattern was observed for MBF (SLR 0.68 ± 0.18), whereas late ^{13}N-NH$_3$ uptake showed a homogeneous distribution (SLR 0.96 ± 0.13). ^{13}N-NH$_3$/^{18}F-FDG ''mismatch'' and ''reverse mismatch'' segments were predominantly present in the lateral (52%) and septal wall (61%), respectively.**

Conclusions. **Non-ischemic CRT candidates with LBBB demonstrate lower glucose uptake and absolute MBF in the septum compared to the lateral wall. However, late static ^{13}N-NH$_3$ uptake showed a homogenous distribution, reflecting a composite measure of altered regional MBF and metabolism, induced by LBBB. (J Nucl Cardiol 2021;28:1730–9.)**

Key Words: PET • myocardial blood flow • dyssynchrony • viability • metabolism imaging agents • perfusion agents

Electronic supplementary material The online version of this article (https://doi.org/10.1007/s12350-019-01900-y) contains supplementary material, which is available to authorized users.

The authors of this article have provided a PowerPoint file, available for download at SpringerLink, which summarizes the contents of the paper and is free for re-use at meetings and presentations. Search for the article DOI on SpringerLink.com.

Funding This work was supported by a KU Leuven research Grant [OT/12/084].

Reprint requests: Ganna Degtiarova, MD, Department of Imaging and Pathology, KU Leuven, Leuven, Belgium; *ganna.degtiarova@kuleuven.be*

1071-3581/$34.00

Abbreviations	
1(2)CM	One(two)-tissue compartment kinetic model
CRT	Cardiac resynchronization therapy
^{18}F-FDG	^{18}F-fluorodeoxyglucose
LV	Left ventricle
LBBB	Left bundle branch block
MBF	Myocardial blood flow
PET	Positron emission tomography
SLR	Septal-to-lateral wall ratio
SUV	Standardized uptake value
TAC	Time-activity curve

See related editorial, pp. 1740–1744

INTRODUCTION

Left bundle branch block (LBBB) is characterized by inhomogeneous activation of the ventricular myocardium resulting in inefficient contraction of the left chamber. Being a risk factor for the development and progression of adverse remodeling and heart failure, LBBB is associated with an increased risk of all-cause mortality.[1] Even though cardiac resynchronization therapy (CRT) is a promising therapy for heart failure patients with LBBB, a significant number of patients do not respond to this therapy, and establishing optimal selection criteria for CRT candidates is still an area of active investigation. Deeper insights into the pathophysiological changes induced by or related to LBBB is needed in order to assess the complex mechanism of disease progression, including causes of adverse remodeling, changes in perfusion, metabolism, and their relation with regard to CRT response or failure.

^{18}F-fluorodeoxyglucose (^{18}F-FDG) positron emission tomography (PET) studies, both quantitative and semiquantitative, in patients with LBBB have shown regional changes in glucose metabolism with a relatively low glucose uptake in the septum and high in the lateral wall.[2,3] These findings correlated with regional differences in myocardial mechanics and structure, as evaluated by cardiac magnetic resonance imaging (CMR) and correspond to the regional redistribution of myocardial work, as assessed with echocardiographic strain techniques.[3,4]

In contrast to the well-established changes in glucose uptake, data on myocardial perfusion in LBBB patients remain controversial. Experimental data have consistently shown a relative hypoperfusion in the septal wall compared to the lateral wall, while clinical nuclear studies predominantly reported a rather homogeneous tracer uptake across the left ventricle (LV) with few studies showing septal hypoperfusion.[2,5]

Identification of different perfusion-metabolism patterns with PET, widely implemented in clinical practice for the assessment of myocardial viability, has been challenging in LBBB patients. It has been demonstrated that ''mismatch''/''reverse mismatch'' patterns can be present in LBBB/CRT eligible patients irrespective of the presence of myocardial hibernation and might have a value in the prediction of CRT response.[6]

Therefore, we investigated the effect of LBBB on regional absolute ^{13}N-NH_3 myocardial perfusion, semi-quantitative late ^{13}N-NH_3 uptake, and ^{18}F-FDG uptake as well as their relation in a homogenous group of patients with non-ischemic dilated cardiomyopathy eligible for CRT.

MATERIAL AND METHODS

Study Population

Patients with non-ischemic heart failure and LBBB (according to the Strauss criteria), referred for CRT implantation, were recruited at the University Hospital Leuven from the Leuven cohort of patients of the WORK-CRT study (Clinical trials NCT02537782). Inclusion for CRT was based on the current ESC criteria.[7] Coronary artery disease was excluded by CMR and/or coronary angiography obtained no more than 3 months before CRT implantation. Exclusion criteria were presence of right bundle branch block, permanent atrial fibrillation, flutter or tachycardia (> 100 bpm), difficulties to obtain LV volumes by echocardiography, history and findings suggestive of ischemic myocardial disease, valve surgery within 90 days prior to enrolment, history of heart transplantation or presence of the patient on the heart transplantation list, implanted LV assist device, severe aortic stenosis, complex and uncorrected congenital heart disease, pregnant and breastfeeding women, enrollment in one or more concurrent studies that would confound the results of this study. The study was approved by the institutional ethics committee and all patients gave written and informed consent prior to inclusion.

PET Acquisition Protocol

All patients underwent resting ^{13}N-NH_3 and ^{18}F-FDG PET studies (Biograph HiRez 16 PET/CT, Siemens, Erlangen, Germany) 1 week before CRT implantation (except for one patient that underwent a ^{99m}Tc-tetrofosmin perfusion scintigraphy). A scout acquisition followed by a low-dose CT (80 kVp, 11 mAs) was performed before each PET emission for optimal patient positioning and subsequent CT-based attenuation correction.

For ^{13}N-NH_3 PET, a slow bolus intravenous administration of 10 MBq kg^{-1} ^{13}N-NH_3 was performed and a 30-minute dynamic list-mode acquisition was started together with radiotracer injection. In case of a one-day protocol, ^{13}N-NH_3 always preceded ^{18}F-FDG imaging with a minimal 60-min interval between tracer administrations.

^{18}F-FDG PET was performed using the euglycemic hyperinsulinemic clamp technique in accordance with the method of Lewis et al.[8] After plasma glucose levels achieved a plateau, 4.25 MBq kg^{-1} ^{18}F-FDG was administered intravenously and a 40-minute ECG-gated acquisition was performed approximately 45 minutes after tracer administration.

Image Processing

Before image reconstruction, alignment between PET and CT images was evaluated and manual realignment was performed if deemed necessary by the investigator. All PET images were reconstructed using ordered-subset expectation maximization algorithms (4 iterations and 8 subsets), matrix size 256 × 256, 5.0 mm Gaussian filter and corrected for attenuation using the low-dose CT.

^{18}F-FDG PET static images, both gated and non-gated, were generated from the whole 40-min acquisition. For ECG-gated reconstructions that included 8 gates, the end-systolic gate was used based on previous results from our group.[9] ^{13}N-NH_3 list-mode file was rebinned into 22 frames (12 frames × 10 seconds, 4 frames × 30 seconds, 3 frames × 120 seconds, 1 frame × 180 seconds, 1 frame 420 seconds, and 1 frame × 600 seconds). The last 20-minute frame was used to analyze ^{13}N-NH_3 late uptake.

PET Image Analysis

All reconstructed ^{13}N-NH_3 and ^{18}F-FDG PET images were analyzed using in-house developed software.[10] Briefly, each myocardial image was resampled into 16 radial slices and a polar map was generated according to previously validated methods.[10] The subsequent analysis was performed both on a segmental and regional level. For segmental analysis, the LV was divided into 17-segment American Heart Association model, but segment 17 was not included for further analysis (Supplemental Figure 1). For regional/wall analysis, LV polar map was divided into 4 regions corresponding to the septal, lateral, anterior, and inferior wall (Supplemental Figure 1).

Regional quantification of myocardial blood flow with ^{13}N-NH_3 Absolute quantification of myocardial blood flow (MBF) was performed per region by modeling the 10- and 2-minute time-activity curves of ^{13}N-NH_3 uptake using a two-tissue (2CM) and one tissue compartment model (1CM), respectively.[11,12] Estimated rate constants were calculated using a weighted least-square method and were corrected for partial-volume effect and spillover, as previously reported.[11] Because the amount of ^{13}N-NH_3 metabolites is known to be negligible during the first 2 minutes after tracer administration, metabolite correction (based on time-metabolite curves from a previous study[13]) was only performed for the 2CM kinetic modeling.

Regional late ^{13}N-NH_3 and ^{18}F-FDG uptake Regional ^{13}N-NH_3 and ^{18}F-FDG uptake were expressed as mean standardized uptake values (SUV). Septal-to-lateral wall ratios (SLR) were calculated by dividing mean uptake in the septum by mean uptake in the lateral wall.

Segmental perfusion-metabolism relation The segmental perfusion-metabolism relation was evaluated using a method that is routinely used to assess myocardial viability. In brief, segmental ^{18}F-FDG uptake was expressed as percentage of the segment with the highest mean late ^{13}N-NH_3 uptake, assuming that the segment with the highest ''perfusion'' should have normal metabolism. Segmental ''reverse mismatch,'' ''mismatch,'' and ''match'' patterns between ^{13}N-NH_3 uptake and ^{18}F-FDG metabolism were defined as ^{13}N-NH_3/^{18}F-FDG uptake ratio $\geq$ 1.2, $\leq$ 0.8 and 0.8-1.2, respectively.[14]

Statistical Analysis

Statistical analysis was performed using SPSS Statistics 20 (IBM, Chicago, IL, USA). Shapiro-Wilk test was used to check the normality of data distribution. Continuous variables are presented as mean ± standard deviation, and categorical variables are presented as percentages. Comparison between septal, lateral, anterior, and inferior walls was performed using one-way ANOVA test with Bonferroni post hoc correction. T test was used for comparison of continuous variables and contingency tables for categorical variables. The correlation between parameters was assessed with Pearson correlation coefficients for normally distributed data; otherwise, Spearman coefficient was used. Comparison of 1CM and 2CM-derived MBF was performed with Bland-Altman analysis. All statistical tests were 2-tailed. A P value of less than 0.05 was considered as statistically significant.

RESULTS

Patient Characteristics

Twenty-five patients (mean age 67 ± 10 years, 13 (52%) males) were included in the study. Three patients

had suboptimal quality of their ^{18}F-FDG scans and 1 patient underwent SPECT ^{99m}Tc-sestamibi scan instead of ^{13}N-NH_3 PET scan. After excluding these studies from the analysis, 22 patients remained with an ^{18}F-FDG PET and 24 with an ^{13}N-NH_3 PET, with 21 patients having had both PET imaging protocols successfully completed.

All patients had stable sinus rhythm. Clinical characteristics of patients are represented in Table 1.

Regional ^{18}F-FDG Uptake

Regional ^{18}F-FDG uptake on gated and non-gated images revealed a similar pattern of tracer distribution, with higher SUVmean values on gated acquisitions, predominantly in the lateral wall (Figure 1). Because no statistically significant difference was observed between the gated and non-gated derived regional ^{18}F-FDG uptake, non-gated ^{18}F-FDG images were used for subsequent analysis.

Table 1. Clinical characteristics of patients

Parameter	All patients (n = 25)
Male (% of total)	13 (52%)
Age (year)	67 ± 10
Diabetes mellitus (% of total)	3 (12%)
Blood pressure	
Systolic blood pressure (mmHg)	135 ± 21
Diastolic blood pressure (mmHg)	70 ± 16
Left ventricular function	
EDV (mL)	162 ± 86
ESV (mL)	113 ± 68
EF (%)	33 ± 8
NYHA class	
NYHA 1	0 (0%)
NYHA 2	15 (60%)
NYHA 3	10 (40%)
NYHA 4	0 (0%)
QRS width (ms)	161 ± 13
Medication	
β-blockers	21 (84%)
ACEi/ARB	22 (88%)
Aldosterone antagonists	13 (52%)

ACEi, angiotensin converting enzyme inhibitors; *ARB*, angiotensin-receptor blockers; *EDV*, end-diastolic volume; *ESV*, end-systolic volume; *EF*, ejection fraction.

Regional ^{18}F-FDG uptake was significantly higher in the lateral wall compared to all other walls ($P \leq .01$). A significantly lower ^{18}F-FDG uptake in the septum was noticed compared to all other regions ($P < .05$), except for the inferior wall ($P = .6$). There was no statistically significant difference in ^{18}F-FDG uptake between anterior and inferior walls (Figure 1).

Regional MBF and Late ^{13}N-NH_3 Uptake

Absolute regional MBF derived from 1CM and 2CM ^{13}N-NH_3 kinetic models was strongly correlated (r = .9, $P < .05$) and showed a good agreement on Bland-Altman plot (bias 0.05 mL g^{-1} min^{-1}, 95% limits of agreements from − 0.14 to 0.23 mL g^{-1} min^{-1}) (Supplemental Figure 2).

Mean absolute MBF in the lateral wall was significantly higher, whereas mean absolute septal MBF was significantly lower than in all other walls, when quantified with 2CM (Figure 2A). Similar results for absolute MBF were obtained with a 1CM (Supplemental Figure 3). In contrast to absolute MBF, regional late ^{13}N-NH_3 SUVmean was homogeneously distributed across the LV myocardium ($P = .16$) (Figure 2B). Only a weak overall correlation ($r = .4$, $P < .001$) was found between regional absolute MBF and late ^{13}N-NH_3 SUVmean.

Visual comparison of regional ^{13}N-NH_3 time-activity curves (TACs) demonstrated a different pattern, with

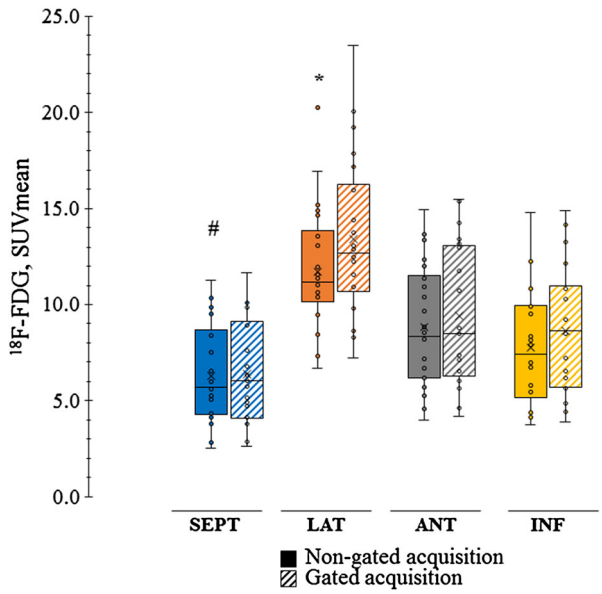

Fig. 1. Regional ^{18}F-FDG uptake. Regional ^{18}F-FDG uptake derived from cardiac gated and non-gated images. *SEPT*, septum; *LAT*, lateral wall; *ANT*, anterior wall; *INF*, inferior wall, $^{*}P \leq .01$ compared to all other walls, $^{\#}P < .05$ compared to the lateral and anterior wall.

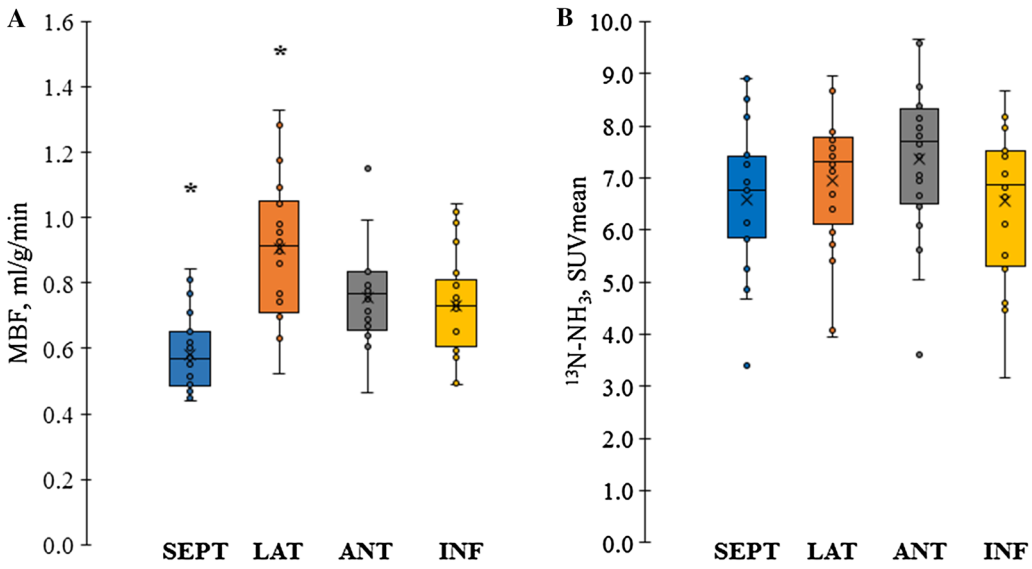

Fig. 2. Regional absolute MBF and late ^{13}N-NH$_3$ uptake. Regional myocardial blood flow (MBF), derived from 2CM kinetic model (**A**) and late ^{13}N-NH$_3$ uptake (**B**) in patients with LBBB. Note, the heterogeneous distribution of absolute perfusion across LV regions (**A**) vs homogeneous regional late ^{13}N-NH$_3$ uptake (**B**). *SEPT*, septum; *LAT*, lateral wall; *ANT*, anterior wall; *INF*, inferior wall, *$P \leq .01$ compared to all other walls.

a plateau in the lateral wall compared to a steadily increased tracer accumulation in the other walls (Figure 3A).

Detailed analysis of regional ^{13}N-NH$_3$ SUVmean changes between 3 and 30 min post tracer administration demonstrated a significant increase in tracer accumulation in the septum (5.42 ± 1.17 vs 6.55 ± 1.35, $P < .01$), anterior (6.61 ± 1.38 vs 7.23 ± 1.43, $P < .01$), and inferior (5.80 ± 1.31 vs 6.47 ± 1.43, $P < .01$) walls, while no significant changes were observed in the lateral wall (6.82 ± 1.36 vs 6.84 ± 1.27, $P = .9$). The temporal changes in SUV were most pronounced in the septal wall, with a 21% increase in tracer accumulation during the 30-min acquisition period, while smaller changes were observed in the lateral, anterior, and inferior wall with, respectively, + 0.2%, + 9% and + 11%. The differences between the temporal changes in ^{13}N-NH$_3$ uptake reached the significance level only between septal and lateral wall ($P = .01$) (Figure 3B).

Septal-to-Lateral Absolute MBF, Late ^{13}N-NH$_3$, and ^{18}F-FDG Uptake Ratios

Mean absolute 2CM-MBF SLR, late ^{13}N-NH$_3$ SLR, and ^{18}F-FDG SLR are represented in Figure 4. ^{18}F-FDG SLR was significantly lower compared to absolute MBF SLR and late ^{13}N-NH$_3$ SLR (0.53 ± 0.17 vs 0.68 ± 0.18 vs 0.96 ± 0.13, respectively, $P \leq .01$). The significantly lower resting absolute MBF in the septum compared to the lateral wall with MBF SLR of 0.68 ± 0.18 was no longer observed on late ^{13}N-NH$_3$ uptake (SLR 0.96 ± 0.13), indicating a more homogenous distribution of ^{13}N-NH$_3$ in the LV. There was a significant but moderate correlation between ^{18}F-FDG and late ^{13}N-NH$_3$ SLR (r = .55, $P = .01$).

Segmental Perfusion-Metabolism Relation

Overall segmental analysis of perfusion-metabolism relation revealed ''mismatch,'' ''reverse mismatch,'' and ''match'' patterns in 70 (21%), 111 (33%), and 155 (46%) segments, respectively.

''Mismatch'' pattern was observed in 3 (3%), 55 (52%), 6 (10%), and 6 (10%) segments in the septum, lateral, anterior, and inferior wall, respectively. ''Reverse mismatch'' patterns in these regions corresponded to 64 (61%), 0 (0%), 25 (40%), and 22 (35%) segments, respectively (Figure 5).

DISCUSSION

The main finding of our study is the presence of regional heterogeneity in glucose metabolism and perfusion with lower glucose uptake and absolute MBF in the septum compared to the lateral wall in non-ischemic CRT candidates with LBBB. In contrast, late ^{13}N-NH$_3$ uptake did not show significant regional differences,

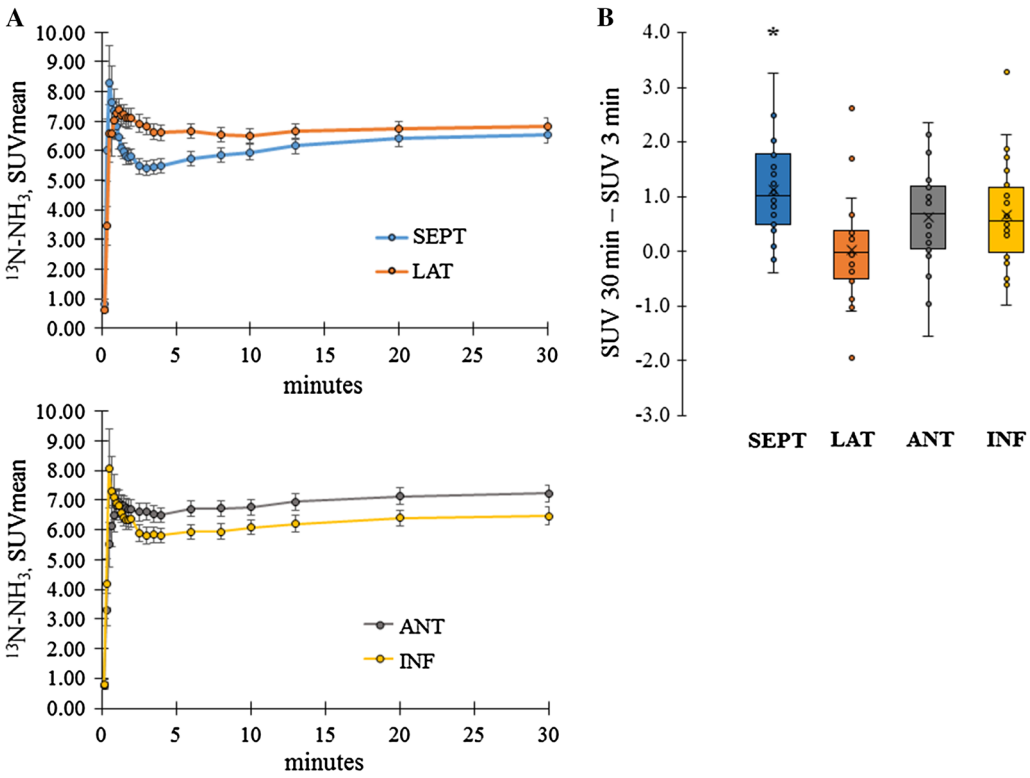

Fig. 3. Regional temporal ^{13}N-NH$_3$ kinetics. Regional time-activity curves, representing changes in mean ^{13}N-NH$_3$ SUV as a function of time (**A**) and regional changes in ^{13}N-NH$_3$ SUV between 3 and 30 min post injection (**B**) in all patients with LBBB. Vertical bars in figure A represent the standard error. *SEPT*, Septum; *LAT*, lateral wall; *ANT*, anterior wall; *INF*, inferior wall, *$P < .01$ compared to the lateral wall.

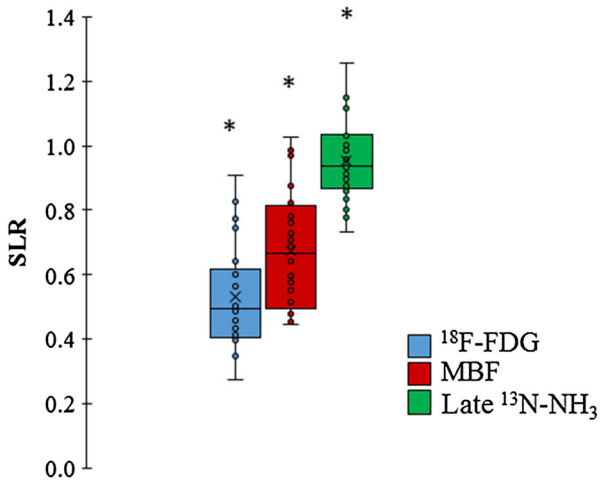

Fig. 4. Septal-to-lateral ratios. Mean septal-to-lateral ^{18}F-FDG, absolute 2CM-MBF, and ^{13}N-NH$_3$ late uptake ratios (SLR). *$P \leq .01$ compared to other SLRs.

hence being a poor parameter for MBF but rather reflecting a composite measure of altered regional MBF and metabolism, induced by LBBB.

Several studies have demonstrated regional changes in glucose metabolism in the presence of LBBB. Among those, an experimental study of Ono et al. showed a significantly lower ^{18}F-FDG uptake in the septum compared to the lateral wall (67.4 ± 12.1% vs 88.0 ± 5.2%, $P < .05$) in right ventricular pacing-induced LBBB. Similar findings were reported in a clinical study of Nowak et al. in patients with LBBB with lowest ^{18}F-FDG uptake in the septum (56 ± 12%), highest in the lateral wall (89 ± 6%), and intermediate values in the anterior and inferior wall (66 ± 12% and 69 ± 8%, respectively).[2,15] The low ^{18}F-FDG SLR in dyssynchronous hearts were also postulated by Neri et al. (0.59 ± 0.17) and Nowak et al. (0.62 ± 0.12).[2,16] Our results are in line with above-mentioned papers, demonstrating a heterogeneous regional glucose metabolism in non-ischemic LBBB heart failure patients with lowest ^{18}F-FDG uptake in the septum, highest in the lateral wall, and intermediate ^{18}F-FDG values in anterior and inferior wall. Furthermore, ^{18}F-FDG SLR obtained in our study (0.53 ± 0.17) perfectly matches the range shown by other groups.

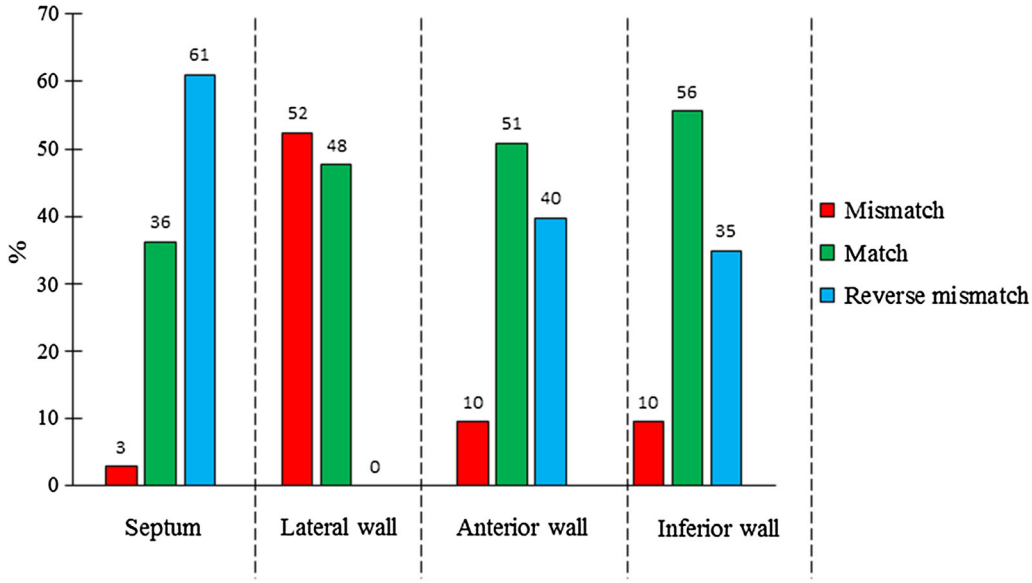

Fig. 5. Perfusion-metabolism patterns. Distribution of late ^{13}N-NH$_3$/^{18}F-FDG ''reverse mismatch,'' ''mismatch,'' and ''match'' patterns between septal, lateral, anterior, and inferior wall.

Such a heterogeneous regional ^{18}F-FDG uptake in patients with LBBB, presented in our and previous studies, can be explained by the fact that the early activated septum does not contribute much to LV contraction or is even wasting work due to systolic stretching, whereas the lateral wall bears most of the load and compensates for the septal dysfunction.[4] Earlier work by our group in a preclinical sheep model has shown that ^{18}F-FDG uptake is linearly correlated with the amount of work performed by the myocardium, which indicates that the observed regional differences in ^{18}F-FDG uptake are an adaptive mechanism to compensate for the difference in regional workload in an asynchronously contracting ventricle.[4]

In contrast to glucose metabolism, findings on regional myocardial perfusion in LBBB patients are controversial. Conflicting results may be attributed among others to different imaging modalities, radiopharmaceuticals, study protocols, and approaches for flow assessment. Earlier studies using SPECT perfusion have shown a decreased perfusion of the septum that can be the result of partial-volume effect in the reported thinned septum, which is less pronounced when recent PET technology is used.[17] Discrepant results for absolute MBF in non-ischemic LBBB patients have also been described with PET depending on the radiotracer used. The study by Baller et al. showed a low absolute MBF for the septum and high MBF for the lateral wall with ^{11}C-acetate, while the study of Koepfli et al. showed a more homogeneous resting perfusion using ^{15}O-water.[18,19] However, in the latter study, stress imaging induced regional perfusion inhomogeneities, which may be explained by the fact that 'stress' increases mechanical dyssynchrony resulting in regional perfusion changes.[20] Additionally, exercise leads to an increased oxygen demand mainly in the extensively working lateral wall leading to a more distinct redistribution of myocardial flow. In our study, regional differences in absolute MBF were similar to metabolic changes, with a low perfusion in the septum, high values in the lateral wall, and intermediate values in anterior and inferior wall. It is unlikely that this difference can be explained by differential partial-volume effects since we did not observe a significant difference in septal and lateral wall thickness (6.99 ± 1.64 mm vs 6.62 ± 1.55 mm, respectively, P = .36) as assessed with CMR in 21 out of 25 patients.

In contrast to our study, Masci et al. reported a rather homogeneous ^{13}N-NH$_3$-derived MBF between septal and lateral walls.[3] One of the possible explanations for their findings could be the exclusion of patients with advanced disease, allowing to assume that LV dyssynchrony was not pronounced enough to induce perfusion heterogeneities. Another explanation could be the different modeling approach to obtain absolute perfusion values. The authors used a simplified perfusion model proposed by Bellina et al., in which absolute MBF is not quantified by fitting a kinetic model to the TAC, but is derived from a fixed myocardial ^{13}N-NH$_3$ concentration measured at a particular time point.[21] Consequently, this derived MBF is always proportional to the tracer uptake at that time point. In our study, we have demonstrated that late ^{13}N-NH$_3$ uptake is

homogeneously distributed between all LV regions and, therefore, when absolute MBF is computed with this simplified model, MBF will also be homogeneous across the regions. In our study, perfusion quantification was performed using a richer kinetic model (full 1CM and 2CM models) which does not impose the perfusion to be proportional to the late myocardial tracer concentration. This can explain the different regional patterns for absolute MBF distribution between both studies.

We hypothesize that perfusion heterogeneity in LBBB patients observed in our study is an example of coronary autoregulation where redistribution of local myocardial workload is associated with similar changes in oxygen demand, hence alterations in blood supply. Differences in regional workload and imbalance in oxygen consumption in asynchronously contracting ventricles have been demonstrated with highest values in the lateral wall and lowest in the septum, which may support the theory of a functional rather than structural adaptive mechanism.[15,22]

In contrast to the regional differences in absolute MBF, late ^{13}N-NH_3 uptake was homogeneously distributed across the LV in our study. These findings correspond with other ^{13}N-NH_3 PET studies in patients with LBBB reporting an average late ^{13}N-NH_3 SLR in the order of one.[23] Earlier reports have demonstrated that ^{13}N-NH_3 fixation in the heart occurs mainly through its ATP-dependent conversion into glutamine via the glutamate-glutamine pathway.[24] The latter suggests a particular role of myocardial metabolism for ^{13}N-NH_3 incorporation which is further supported by the significant, even though moderate, correlation between late ^{13}N-NH_3 and ^{18}F-FDG SLR is observed in our study. Furthermore, our and other studies did not show a perfect linear correlation between MBF and late ^{13}N-NH_3 uptake, illustrating that late ^{13}N-NH_3 myocardial uptake is rather a combined assessment of MBF and metabolism.[25] The latter is supported by the study of Choi et al. reporting ^{13}N-NH_3 SUV to be a poor indicator of MBF by comparing six different methods for the assessment of myocardial perfusion in dogs and healthy volunteers.[26]

The different regional temporal kinetics of ^{13}N-NH_3 shown in our study with a plateau in the lateral wall and steadily increased tracer accumulation in the rest of the heart is not fully understood, but explains the homogenous late ^{13}N-NH_3 uptake despite significant differences in absolute MBF. One of the possible hypotheses for the different regional ^{13}N-NH_3 kinetics between myocardial walls can be linked to regional metabolic alterations secondary to functional adaptive mechanisms, with different levels of glutamate, glutamate synthetase, free available ATP, intracellular level of NH_3, intracellular pH, that all may play a role in myocardial tracer fixation. However, further studies are needed to fully understand and explain the observed regional differences.

Finally, a differential relation between perfusion and metabolism in septal and lateral walls characterized as ''mismatch'' and ''reverse mismatch'' patterns using a common method for viability assessment has been shown in LBBB patients in our study. Similarly to the study of Masci et al., ''mismatch'' segments were predominantly present in the lateral wall (52%), while ''reverse mismatch'' segments were mainly observed in the septum (61%).[3] The presence of these perfusion/metabolism ''mismatch'' and ''reverse mismatch'' patterns in LBBB patients are most likely attributed to the physiological changes induced by the presence of LBBB and should be taken into account when patients with LBBB are referred for viability assessment prior to revascularization procedures. In addition, further investigations are needed to evaluate whether specific perfusion/metabolism patterns in LBBB patients may predict response to CRT; however, one study has shown that the presence of reverse mismatch patterns in the septum was associated with good prognosis after.[6]

Our study had several limitations. Although ischemia was excluded in our patient cohort based on CMR and/or coronary angiography 3 months prior to CRT implantation, one cannot completely rule out ischemia at the time of CRT implantation; however, these chances are negligible. In the current study, clinically used reconstruction algorithms and software programs were applied without correcting for partial-volume effect, which may lead to a slight underestimation of the true tracer concentration in the thinned walls. Furthermore, we did not perform absolute quantification of cardiac glucose metabolism, but only mean glucose uptake defined by SUV was used in the current study. Quantification of glucose consumption as well as using other metabolic PET tracers such as ^{11}C-acetate could help to better understand the pathophysiological mechanisms and metabolic adaptations during abnormal LV activation patterns. The presence of a comparable control group with non-ischemic cardiomyopathy without LV dyssynchrony would have been informative to define whether the alterations observed in myocardial perfusion and metabolism in non-ischemic LBBB patients are absolute or rather relative. This control group would also provide more insights into the temporal kinetics of ^{13}N-NH_3 uptake in different walls to further support the assumption that the different regional temporal kinetics are attributed to abnormal LV activation.

NEW KNOWLEDGE GAINED

The presence of LBBB in non-ischemic CRT candidates is associated with heterogeneity in regional glucose metabolism and MBF, with a significant lower SLR for ^{18}F-FDG compared to absolute MBF.

In non-ischemic CRT candidates with LBBB, there is only a weak correlation between absolute MBF and late ^{13}N-NH_3 uptake, proving that late ^{13}N-NH_3 is a composite of perfusion and metabolism with regional differences most likely caused by LV dyssynchrony.

CONCLUSIONS

Non-ischemic heart failure patients with LBBB demonstrate lower myocardial glucose uptake and absolute MBF in the septum compared to the lateral wall. However, late static ^{13}N-NH_3 uptake did not show significant regional differences, demonstrating that there is no perfect correlation between absolute MBF and late ^{13}N-NH_3 with the latter being a composite measure of absolute MBF and myocardial metabolism. Regional differences in temporal ^{13}N-NH_3 kinetics in LBBB patients are present but further investigations are warranted to elucidate the underlying pathophysiological mechanism.

Disclosures

All authors report no relationships that could be construed as a conflict of interest.

References

1. Hesse B, Diaz LA, Snader CE, Blackstone EH, Lauer MS. Complete bundle branch block as an independent predictor of all-cause mortality: Report of 7,073 patients referred for nuclear exercise testing. Am J Med 2001;110:253-9.
2. Nowak B, Sinha AM, Schaefer WM, Koch KC, Kaiser HJ, Hanrath P, et al. Cardiac resynchronization therapy homogenizes myocardial glucose metabolism and perfusion in dilated cardiomyopathy and left bundle branch block. J Am Coll Cardiol 2003;41:1523-8.
3. Masci PG, Marinelli M, Piacenti M, Lorenzoni V, Positano V, Lombardi M, et al. Myocardial structural, perfusion, and metabolic correlates of left bundle branch block mechanical derangement in patients with dilated cardiomyopathy: A tagged cardiac magnetic resonance and positron emission tomography study. Circ Cardiovasc Imaging 2010;3:482-90.
4. Duchenne J, Turco A, Ünlü S, Pagourelias ED, Vunckx K, Degtiarova G, et al. Left ventricular remodeling results in homogenization of myocardial work distribution. Circ Arrhythmia Electrophysiol 2019;12:1-14.
5. Vernooy K, Verbeek XAAM, Peschar M, Crijns HJGM, Arts T, Cornelussen RNM, et al. Left bundle branch block induces ventricular remodelling and functional septal hypoperfusion. Eur Heart J 2005;26:91-8.
6. Inoue N, Takahashi N, Ishikawa T, Sumita S, Kobayashi T, Matsushita K, et al. Reverse perfusion-metabolism mismatch predicts good prognosis in patients undergoing cardiac resynchronization therapy: A pilot study. Circ J 2007;71:126-31.
7. European Society of Cardiology (ESC), European Heart Rhythm Association (EHRA), Brignole M, Auricchio A, Baron-Esquivias G, Bordachar P, et al. 2013 ESC guidelines on cardiac pacing and cardiac resynchronization therapy: The task force on cardiac pacing and resynchronization therapy of the European Society of Cardiology (ESC). Developed in collaboration with the European Heart Rhythm Association. Europace 2013;15:1070-118.
8. Lewis P, Nunan T, Dynes A, Maisey M. The use of low-dose intravenous insulin in clinical myocardial F-18 FDG PET scanning. Clin Nucl Med 1996;21:15-8.
9. Turco A, Gheysens O, Duchenne J, Nuyts J, Rega F, Voigt JU, et al. Partial volume and motion correction in cardiac PET: First results from an in vs ex vivo comparison using animal datasets. J Nucl Cardiol 2019. https://doi.org/10.1007/s12350-018-01581-z.
10. Nuyts J, Suetens P, Oosterlinck A, De Roo M, Mortelmans L. Delineation of ECT images using global constraints and dynamic programming. IEEE Trans Med Imaging 1991;10:489-98.
11. Hutchins GD, Schwaiger M, Rosenspire KC, Krivokapich J, Schelbert H, Kuhl DE. Noninvasive quantification of regional blood flow in the human heart using N-13 ammonia and dynamic positron emission tomographic imaging. J Am Coll Cardiol 1990;15:1032-42.
12. DeGrado TR, Hanson MW, Turkington TG, Delong DM, Brezinski DA, Vallée JP, et al. Estimation of myocardial blood flow for longitudinal studies with 13N-labeled ammonia and positron emission tomography. J Nucl Cardiol 1996;3:494-507.
13. Bormans G, Maes A, Langendries W, Nuyts J, Vrolix M, Vanhaecke J, et al. Metabolism of nitrogen-13 labelled ammonia in different conditions in dogs, human volunteers and transplant patients. Eur J Nucl Med 1995;22:116-21.
14. Flameng WJ, Shivalkar B, Spiessens B, Maes A, Nuyts J, VanHaecke J, et al. PET scan predicts recovery of left ventricular function after coronary artery bypass operation. Ann Thorac Surg 1997;64:1694-701.
15. Ono S, Nohara R, Kambara H, Okuda K, Kawai C. Regional myocardial perfusion and glucose metabolism in experimental left bundle branch block. Circulation 1992;85:1125-31.
16. Neri G, Zanco P, Zanon F, Buchberger R. Effect of biventricular pacing on metabolism and perfusion in patients affected by dilated cardiomyopathy and left bundle branch block: Evaluation by positron emission tomography. Europace 2003;5:111-5.
17. Nowak B, Stellbrink C, Schaefer WM, Sinha AM, Breithardt OA, Kaiser H-J, et al. Comparison of regional myocardial blood flow and perfusion in dilated cardiomyopathy and left bundle branch block: Role of wall thickening. J Nucl Med 2004;45:414-8.
18. Baller D, Vogt J, Lindner O, Lamp B, Holzinger J, Kammeier A, et al. Myocardial oxygen consumption and perfusion before and after cardiac resynchronization therapy: Experimental observations and clinical implications. Eur Hear J 2004;6:D91-7.
19. Koepfli P, Wyss CA, Gaemperli O, Siegrist PT, Klainguti M, Schepis T, et al. Left bundle branch block causes relative but not absolute septal underperfusion during exercise. Eur Heart J 2009;30:2993-9.
20. Stankovic I, Aarones M, Smith H-J, Vörös G, Kongsgaard E, Neskovic AN, et al. Dynamic relationship of left-ventricular dyssynchrony and contractile reserve in patients undergoing cardiac resynchronization therapy. Eur Heart J 2014;35:48-55.
21. Bellina CR, Parodi O, Camici P, Salvadori PA, Taddei L, Fusani L, et al. Simultaneous in vitro and in vivo validation of nitrogen-13-ammonia for the assessment of regional myocardial blood flow. J Nucl Med 1990;31:1335-43.
22. Knaapen P, van Campen LM, de Cock CC, Götte MJW, Visser CA, Lammertsma AA, et al. Effects of cardiac resynchronization therapy on myocardial perfusion reserve. Circulation 2004;110:646-51.

23. Zanco P, Desideri A, Mobilia G, Cargnel S, Milan E, Celegon L, et al. Effects of left bundle branch block on myocardial FDG PET in patients without significant coronary artery stenoses. J Nucl Med 2000;41:973-7.
24. Schelbert HR, Phelps ME, Huang SC, MacDonald NS, Hansen H, Selin C, et al. N-13 ammonia as an indicator of myocardial blood flow. Circulation 1981;63:1259-72.
25. Shah A, Schelbert HR, Schwaiger M, Henze E, Hansen H, Selin C, et al. Measurement of regional myocardial blood flow with N-13 ammonia and positron-emission tomography in intact dogs. J Am Coll Cardiol 1985;5:92-100.
26. Choi Y, Huang SC, Hawkins RA, Kim JY, Kim BT, Hoh CK, et al. Quantification of myocardial blood flow using 13N-ammonia and PET: Comparison of tracer models. J Nucl Med 1999;40:1045-55.